Inorg. Chem. **2005**, *44*, 8433–8441

Synthesis, Structure, and Magnetic Ordering of Layered (2-D) V-Based Tris(oxalato)metalates

Kil Sik Min,[1a] Arnold L. Rhinegold,[1b] and Joel S. Miller*,[1a]

Departments of Chemistry, University of Utah, 315 South 1400 East, Room 2020, Salt Lake City, Utah 84112-0850, and University of California, San Diego, 9500 Gilman Drive, La Jolla, California 92093

Received August 11, 2005

The reaction of $K_3[M^{III}(ox)_3]\cdot 3H_2O$ [M = V (**1**), Cr; ox = oxalate], Mn(II)/V(II), and $[N(n\text{-}Bu)_4]Br$ in water leads to the isolation of 2-D V-based coordination polymers, $\{[N(n\text{-}Bu)_4][Mn^{II}V^{III}(ox)_3]\}_n$ (**2**), $\{[N(n\text{-}Bu)_4][V^{II}Cr^{III}(ox)_3]\}_n$ (**3**), $\{[N(n\text{-}Bu)_4][V^{II}V^{III}(ox)_3]\}_n$ (**4**), and an intermediate in the formation of **4**, $\{[N(n\text{-}Bu)_4][V^{II}V^{III}(ox)_3(H_2O)_2]\}_n\cdot 2.5H_2O$ (**4a**), while 1-D $[V^{II}(ox)(H_2O)_2]_n$ (**5**) is obtained by using Na_2ox and $[V(OH_2)_6]SO_4$ in water. The structures of **1**–**5** have been investigated by single crystal and/or powder X-ray crystallography. In **1**, V^{III} is coordinated with three oxalate dianions as an approximately D_3 symmetric, trigonally distorted octahedron. **1** is paramagnetic [μ_{eff} = 2.68 μ_B at 300 K, D = 3.84 cm^{-1} (D/k_B = 5.53 K), θ = –1.11 K, and g = 1.895], indicating an S = 1 ground state. **2** exhibits intralayer ferromagnetic coupling below 20 K, but does not magnetically order above 2 K, and **3** shows a strong antiferromagnetic interaction between V^{II}, S = 3/2 and Cr^{III}, S = 3/2 ions (θ = –116 K) within the 2-D layers. **4** and **4a** magnetically order as ferrimagnets at T_c's, taken as the onset of magnetization, of 11 and 30 K, respectively. The 2 K remanent magnetizations are 2440 and 2230 emu·Oe mol^{-1} and the coercive fields are 1460 and 4060 Oe for **4** and **4a**, respectively. Both **4** and **4a** clearly show frequency dependence, indicative of spin-glass-like behavior. The glass transition temperatures were at 6.3 and 27 K, respectively, for **4** and **4a**. 1-D **5** exhibits antiferromagnetic coupling of –4.94 cm^{-1} ($H = -2J\sum_{i=1}^{n} S_i\cdot S_{i-1} - g\mu_B\sum_{i=0}^{n} H\cdot S_i$) between the V^{II} ions.

Introduction

The study of magnetically ordered molecule-based magnetic materials is a growing area of contemporary chemistry.[2,3] $[Fe(C_5Me_5)_2]^{\bullet+}[TCNE]^{\bullet-}$ (TCNE = tetracyanoethylene) was the first organic-containing molecule-based magnet, with an ordering temperature, T_c, of 4.8 K,[4] and replacement of S = 1 Mn^{III} for S = 1/2 Fe^{III} led to characterization of $[Mn(C_5Me_5)_2]^{+}[TCNE]^{\bullet-}$ with an 8.8 K T_c.[5] Use of V^{II}, via oxidation of $V^{\circ}(C_6H_6)_2$, led to the discovery of $V(TCNE)_x\cdot y$(solvent), the first room-temperature organic magnet ($T_c \sim$ 400 K).[6] While spin-bearing bridging ligands, such as $[TCNE]^{\bullet-}$, enable extended, strong spin coupling among spin-bearing metal ions, both cyanide and oxalate (ox^{2-}) can

* E-mail: jsmiller@chem.utah.edu.

(1) (a) University of Utah. (b) University of California, San Diego.

(2) (a) Day, P.; Underhill, A. E. Metal-organic and Organic Molecular Magnets. *Philos. Trans. R. Soc. London, Ser. A* **1999**, *357*, 2849–3184. (b) Kahn, O., Ed. Proceedings of the 6th International Conference on Molecule-based Based Materials. *Mol. Cryst. Liq. Cryst.* **1999**, *334/335*. (c) Itoh, K., Miller, J. S., Takui, T., Eds. Proceedings of the Conference on Molecule-Based Magnets. *Mol. Cryst., Liq. Cryst.* **1997**, *305–306*. (d) Christou, G., Ed. Proceedings of the 7th International Conference on Molecule-based Magnets. *Polyhedron* **2001**, *20* (*no. 11–14*). (e) Christou, G., Ed. Proceedings of the 8th International Conference on Molecule-based Magnets. *Polyhedron* **2003**, *22* (*no. 14–17*).

(3) Reviews: (a) Miller, J. S.; Epstein, A. J. *Chem. Commun.* **1998**, 1319. (b) Ovcharenko, V. I.; Sagdeev, R. Z. *Russ. Chem. Rev.* **1968**, *68*, 345. (c) Plass, W. *Chem. Z.* **1998**, *32*, 323. (d) Miller, J. S.; Epstein, A. J. *Chem. Eng. News* **1995**, *73* (*no.* 40), 30. (e) Miller, J. S.; Epstein, A. J. *Angew. Chem., Int. Ed. Engl.* **1994**, *33*, 385. (f) Kinoshita, M. *Jpn. J. Appl. Phys.* **1994**, *33*, 5718. (g) Miller, J. S.; Epstein, A. J. *Adv. Chem. Ser.* **1995**, *245*, 161. (h) Caneschi, A.; Gatteschi, D. *Prog. Inorg. Chem.* **1991**, *37*, 331. (i) Buchachenko, A. L. *Russ. Chem. Rev.* **1990**, *59*, 307. (j) Kahn, O. *Struct. Bonding* **1987**, *68*, 89. (k) Caneschi, A.; Gatteschi, D.; Sessoli, R.; Rey, P. *Acc. Chem. Res.* **1989**, *22*, 392. (l) Gatteschi, D. *Adv. Mater.* **1994**, *6*, 635.

(4) (a) Miller, J. S.; Calabrese, J. C.; Epstein, A. J.; Bigelow, R. W.; Zhang, J. H.; Reiff, W. M. *J. Chem. Soc., Chem. Commun.* **1986**, 1026. (b) Miller, J. S.; Calabrese, J. C.; Rommelmann, H.; Chittipeddi, S.; Zhang, J. H.; Reiff, W. M.; Epstein, A. J. *J. Am. Chem. Soc.* **1987**, *109*, 769.

(5) Yee, G. T.; Manriquez, J. M.; Dixon, D. A.; McLean, R. S.; Groski, D. M.; Flippen, R. B.; Narayan, K. S.; Epstein, A. J.; Miller, J. S. *Adv. Mater.* **1991**, *3*, 309.

(6) (a) Manriquez, J. M.; Yee, G. T.; McLean, R. S.; Epstein, A. J.; Miller, J. S. *Science* **1991**, *252*, 1415. (b) Miller, J. S.; Yee, G. T.; Manriquez, J. M.; Epstein, A. J. *Conjugated Polymers and Related Materials: The Interconnection of Chemical and Electronic Structure*; Proceedings of Nobel Symposium no. NS-81; Oxford University Press: Oxford, 1993; p 461; *Chim. Ind.* **1992**, *74*, 845.

10.1021/ic051373+ CCC: $30.25
Published on Web 10/05/2005

also mediate strong spin coupling between paramagnetic centers separated by more than 5 Å. Hence, hexacyanometalate-based, Prussian blue structured magnets with T_cs as high as ~100 °C,[7,8] and tris(oxalato)chromates(III) and ferrates(III) pioneered by Okawa[9] have been reported.

Magnets based on tris(oxalato)metalate(III) have a general formula of $A[M^{II}M^{III}(ox)_3]$ (A = monovalent cation; M^{II} = Mn, Fe, Ni, Co, Cu, Zn; M^{III} = Cr, Fe, Ru).[9−13] This family of materials has a 2-D honeycomb layered structure, Figure 1, and magnetically order as either ferro- or ferrimagnets depending on the metal ions. T_cs of these materials have shown characteristic ranges depending on the $[M^{III}(ox)_3]^{3-}$ anions, i.e., $\{M^{II}[Cr^{III}(ox)_3]\}^-$ (5−14 K), $\{M^{II}[Fe^{III}(ox)_3]\}^-$ (25−45 K), $\{M^{II}[Ru^{III}(ox)_3]\}^-$ (<14 K). For example, $\{Mn^{II}[Cr^{III}(ox)_3]\}^-$ and $\{Mn^{II}[Fe^{III}(ox)_3]\}^-$ magnetically order at ~6 and ~27 K, as ferro- or ferrimagnets, respectively. Compounds possessing $\{Fe^{II}[Fe^{III}(ox)_3]\}^-$ are ferrimagnets with T_cs between 28 and 45 K, depending on the cation, as well as exhibit an unusual crossover from positive to negative magnetization.[11g] While magnets based upon $[M^{III}(ox)_3]^{3-}$ (M = Cr, Fe) have been extensively studied, $[V^{III}(ox)_3]^{3-}$ has not been explored, due in part to its lability in an aqueous solution.[14] As vanadium-based molecule-based magnets have the highest T_cs,[6,8] we sought magnets based upon $[V^{III}(ox)_3]^{3-}$, as well as $\{V^{II}[M^{III}(ox)_3]\}^-$. Furthermore, V^{III}, having a t_2^2 electronic configuration, like t_2^3 V^{II}, lacks electrons in an antibonding orbital, as occurs for Fe^{III}; hence,

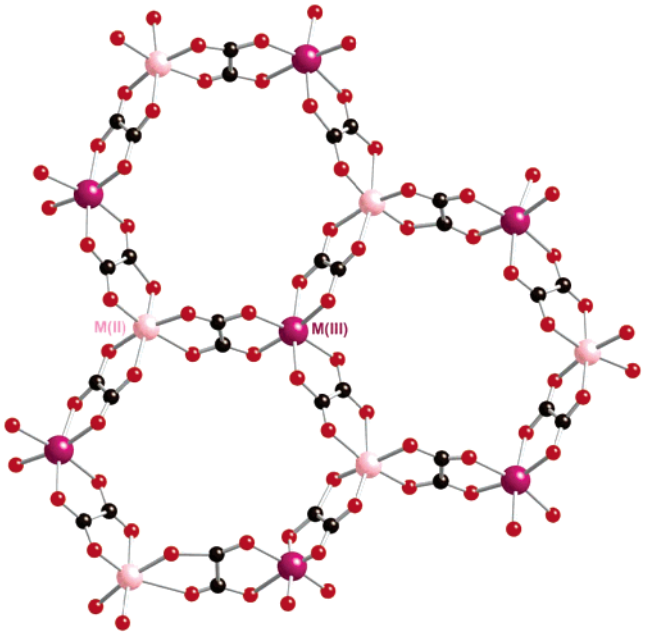

Figure 1. General 2-D honeycomb layered structure of layer of $NBu_4[M^{II}M^{III}(ox)_3]$ (M^{II} = Mn, Fe, Ni, Co, Cu, Zn; M^{III} = Cr, Fe, Ru), and that of **2**, **3**, and **4**.

like $\{M^{II}[Cr^{III}(ox)_3]^{3-}\}$,[9] $\{M^{II}[V^{II}(ox)_3]^{3-}\}$ should order as a ferromagnet, and as an antiferromagnet as occurs for $\{M^{II}[Fe^{III}(ox)_3]^{3-}\}$.[13] Hence, herein we report the structure and magnetic properties of $K_3[V(ox)_3]\cdot 3H_2O$ (**1**), 2-D layered $\{[N(n\text{-}Bu)_4][Mn^{II}V^{III}(ox)_3]\}_n$ (**2**), $\{[N(n\text{-}Bu)_4][V^{II}Cr^{III}(ox)_3]\}_n$ (**3**), $\{[N(n\text{-}Bu)_4][V^{II}V^{III}(ox)_3]\}_n$ (**4**), and $\{[N(n\text{-}Bu)_4][V^{II}V^{III}(ox)_3(H_2O)_2]\}_n\cdot 2.5H_2O$ (**4a**), and 1-D $[V^{II}(ox)(H_2O)_2]_n$ (**5**).

Experimental Section

All chemicals used in the synthesis were of reagent grade and used without further purification. $[V^{II}(OH_2)_6]SO_4$ was synthesized by a literature procedure.[15] $K_3[V(ox)_3]\cdot 3H_2O$ (**1**) was prepared by slightly modified literature procedure:[16] VCl_3 was used instead of V_2O_5, and EtOH was added to precipitate **1**. Solvents were distilled from the appropriate drying agents under nitrogen before use. Aqueous solutions were prepared with water purified through a Barnstead "E-pure" water purification system, deoxygenated through sparging with N_2 for 12 h, and confirmed to be oxygen-free by UV−vis spectroscopic studies. All syntheses were performed in a wet or dry oxygen-free (<0.5 ppm O_2) box. Single crystals of **1** suitable for X-ray crystallography were obtained from a water solution by slow evaporation. Infrared spectra were recorded with a Bruker Tensor 37 FT-IR spectrophotometer. Elemental analyses were performed by the E & R Microanalytical Division of Complete Analysis Laboratories, Inc. X-ray powder diffraction (XRPD) data were recorded on a Bruker AXS diffractometer at 40 kV and 40 mA for Cu Kα (λ = 1.5406 Å) with a scan speed of 0.24°/min and a step size of 0.02° in 2θ. Thermogravimetric analysis (TGA) was performed at a scan rate of 5 °C/min using a TGA 2050 TA instrument located in a Vacuum Atmospheres DriLab under nitrogen to protect air- and moisture-sensitive samples. Samples were placed in an aluminum pan and heated at 5 °C/min under a continuous 10 mL/min nitrogen flow.

(7) (a) Verdaguer, M. et al. *Coord. Chem. Rev.* **1999**, *190−192*, 1023. (b) Verdaguer, M.; Bluezen, A.; Train, C.; Garde, R.; Fabrizi de Biani, F.; Desplanches, C. *Philos. Trans. Soc. London A* **1999**, *357*, 2959. (c) Hashimoto, K.; Ohkoshi, S.-I. *Philos. Trans. Soc. London A* **1999**, *357*, 2977. (d) Verdaguer, M.; Girolami, G. S. In *Magnetism − Molecules to Materials*; Miller, J. S., Drillon, M., Eds.; Wiley-VCH: Mannheim, 2004; Vol. 5, p 283. (e) Miller, J. S. *MRS Bull.* **2000**, *25 (no. 11)*, 60.

(8) (a) Ferlay, S.; Mallah, T.; Ouahes, R.; Veillet, P.; Verdaguer, M. *Nature* **1995**, *378*, 701. (b) Holmes, S. M.; Girolami, G. S. *J. Am. Chem. Soc.* **1999**, *121*, 5593. (c) Hatlevik, Ø.; Buschmann, W. E.; Zhang, J.; Manson, J. L.; Miller, J. S. *Adv. Mater.* **1999**, *11*, 914. (d) Garde, R.; Villain, F.; Verdaguer, M. *J. Am. Chem. Soc.* **2002**, *124*, 10531. (e) Dujardin, E.; Ferlay, S.; Phan, X.; Desplanches, C.; Moulin, C. C. d.; Sainctavit, P.; Baudelet, F.; Dartyge, E.; Veillet, P.; Verdaguer, M. *J. Am. Chem. Soc.* **1998**, *120*, 11347.

(9) (a) Zhong, Z. J.; Matsumoto, N.; Okawa, H.; Kida, S. *Chem. Lett.* **1990**, 87. (b) Tamaki, H.; Zhong, Z. J.; Matsumoto, N.; Kida, S.; Koikawa, M.; Achiwa, N.; Hashimoto, Y.; Okawa, H. *J. Am. Chem. Soc.* **1992**, *114*, 6974.

(10) Descurtins, S. In *Magnetism − Molecules to Materials*; Miller, J. S., Drillon, M., Eds.; Wiley-VCH: Mannheim, 2001; Vol. 2, p 339.

(11) (a) Pellaux, R.; Schmalle, H. W.; Huber, R.; Fischer, P.; Hauss, T.; Ouladdiaf, B.; Decurtins, S. *Inorg. Chem.* **1997**, *36*, 2301. (b) Larionova, J.; Mombelli, B.; Sanchiz, J.; Kahn, O. *Inorg. Chem.* **1998**, *37*, 679. (c) Coronado, E.; Galán-Mascarós, J. R.; Gómez-García, C. J.; Martínez-Agudo, J. M. *Adv. Mater.* **1999**, *11*, 558. (d) Nuttall, C. J.; Day, P. *J. Solid State Chem.* **1999**, *147*, 3. (e) Coronado, E.; Galán-Mascarós, J. R.; Gómez-García, C. J.; Martínez-Agudo, J. M. *Inorg. Chem.* **2001**, *40*, 113. (f) Coronado, E.; Galán-Mascarós, J. R.; Gómez-García, C. J.; Martínez-Agudo, J. M.; Martínez-Ferrero, E.; Waerenborgh, J. C.; Almeida, M. *J. Solid State Chem.* **2001**, *159*, 391. (g) Mathonière, C.; Nuttall, C. J.; Carling, S. G.; Day, P. *Inorg. Chem.* **1996**, *35*, 1201.

(12) Isostructural $A[M^{II}M^{III}(ox)_3]$ (A = NBu^t_4, NMe_4, PPh_4) has also been characterized but due to S = 0 Co(III) does not magnetically order. Sanina, N. A.; Shilov, G. V.; Ovanesyan, N. S.; Atovmyan, L. O. *Russ. Chem. Bull.* **1999**, *48*, 1581.

(13) Tamaki, M.; Mitsumi, M.; Nakamura, K.; Matsumoto, N.; Kida, S.; Okawa, H.; Iijima, S. *Chem. Lett.* **1992**, 1975.

(14) (a) Gillard, R. D.; Laurie, S. H.; Mitchell, P. R. *J. Chem. Soc. (A)* **1969**, 3006. (b) Matsumoto, A.; Kumafuji, H.; Shiokawa, J. *Inorg. Chim. Acta* **1980**, *42*, 149.

(15) Cotton, F. A.; Falvello, L. R.; Llusar, R.; Libby, E.; Murillo, C. A.; Schwotzer, W. *Inorg. Chem.* **1986**, *25*, 3423.

(16) Piccini, A.; Brizzi, N. *Z. Anorg. Chem.* **1899**, *19*, 394.

{[N(*n*-Bu)$_4$][Mn^{II}V^{III}(ox)$_3$]}$_n$ (2). An aqueous solution (10 mL) of $MnCl_2 \cdot 4H_2O$ (395 mg, 2 mmol) was added dropwise to an aqueous solution (10 mL) of $K_3[V(ox)_3] \cdot 3H_2O$ (973 mg, 2 mmol) at room temperature. To the resulting green solution was added an aqueous solution (5 mL) of tetra-*n*-butylammonium bromide (709 mg, 2.2 mmol) to immediately induce a precipitation of green solid. After standing at room temperature for 30 min, the product was collected by filtration, washed with H_2O and EtOH, and dried in vacuo (Yield: 1.05 g; 86%). Anal. Calcd for $C_{22}H_{36}MnNO_{12}V$: C, 43.15; H, 5.93; N, 2.29. Found: C, 43.37; H, 6.11; N, 2.42. FT-IR (KBr): 2970, 2879, 1630 (ν_{CO}), 1446, 1425, 1297, 814, 532, 481 cm^{-1}. The TGA of **2** shows that decomposition starts at 280 °C and occurs abruptly at 345 °C.

{[N(*n*-Bu)$_4$][V^{II}Cr^{III}(ox)$_3$]}$_n$ (3). An aqueous solution (10 mL) of $[V(OH_2)_6]SO_4$ (228 mg, 0.89 mmol) was added dropwise to an aqueous solution (5 mL) of $K_3[Cr(ox)_3] \cdot 3H_2O$ (435 mg, 0.89 mmol) at room temperature. After stirring for 30 min, an aqueous solution (2 mL) of tetra-*n*-butylammonium bromide (317 mg, 0.98 mmol) was added to the resulting dark-violet solution. Upon standing at room temperature for several days, dark-violet **3** formed. It was collected by filtration, washed with H_2O and MeOH, and dried in vacuo (Yield: 163 mg; 30%). Anal. Calcd for $C_{22}H_{36}CrNO_{12}V$: C, 43.36; H, 5.95; N, 2.30. Found: C, 43.19; H, 6.21; N, 2.29. FT-IR (KBr): 2968 (ν_{CH}), 2879 (ν_{CH}), 1619 (ν_{CO}), 1457, 1428, 1294, 807, 541, 472 cm^{-1}. Reaction of Cr^{II} with $K_3[V(ox)_3] \cdot 3H_2O$ also forms **3**. The TGA of **3** shows that decomposition starts at 215 °C and occurs abruptly at 310 °C.

{[N(*n*-Bu)$_4$][V^{II}V^{III}(ox)$_3$]}$_n$ (4). An aqueous solution (3 mL) of $[V(OH_2)_6]SO_4$ (259 mg, 1.02 mmol) was added dropwise to an aqueous solution (6 mL) of $K_3[V(ox)_3] \cdot 3H_2O$ (495 mg, 1.02 mmol) at room temperature. After stirring for 30 min, an aqueous solution (2 mL) of tetra-*n*-butylammonium bromide (361 mg, 1.12 mmol) was added to the resulting dark-brown solution. Upon stirring at room temperature for 3 days, dark-violet **4** formed. It was collected by filtration, washed with H_2O, and dried in vacuo (Yield: 394 mg; 64%). Anal. Calcd for $C_{22}H_{36}NO_{12}V_2$: C, 43.43; H, 5.96; N, 2.30. Found: C, 43.12; H, 5.74; N, 2.22. FT-IR (KBr): 2970 (ν_{CH}), 2880 (ν_{CH}), 1621 (ν_{CO}), 1446, 1420, 1335, 1293, 908, 815, 531, 472 cm^{-1}. The TGA shows that decomposition starts at 220 °C and occurs abruptly at 280 °C.

{[N(*n*-Bu)$_4$][V^{II}V^{III}(ox)$_3$(H$_2$O)$_2$]}$_n \cdot$2.5H$_2$O (4a). An aqueous solution (2 mL) of $[V(OH_2)_6]SO_4$ (255 mg, 1.0 mmol) was added dropwise to an aqueous solution (3 mL) of $K_3[V(ox)_3] \cdot 3H_2O$ (486 mg, 1.0 mmol) at room temperature. After stirring for 20 min, an aqueous solution (2 mL) of tetra-*n*-butylammonium bromide (322 mg, 1.0 mmol) was added to the resulting dark-brown solution. Upon stirring at room temperature for 2 h dark-violet **4a** formed. It was collected by filtration, washed with H_2O, and dried in vacuo (Yield: 90 mg; 16%). Anal. Calcd for $C_{22}H_{45}NO_{16.5}V_2$ {[N(*n*-Bu)$_4$][V^{II}V^{III}(ox)$_3$(H$_2$O)$_2$]}$_n \cdot$2.5H$_2$O:[17] C, 38.32; H, 6.58; N, 2.03. Found: C, 38.12; H, 6.02; N, 2.25. FT-IR (KBr): 3528 (ν_{OH}, br), 2960 (ν_{CH}), 2874 (ν_{CH}), 1624 (ν_{CO}), 1603 (ν_{CO}), 1474, 1345, 1305, 806, 528, 477 cm^{-1}. The TGA shows a weight loss of 5.1% below 250 °C, corresponding to the loss of two water molecules per unit formula. No chemical decomposition was observed up to 260 °C.

[V^{II}(ox)(OH$_2$)$_2$]$_n$ (5). An aqueous solution (10 mL) of Na_2ox (210 mg, 1.57 mmol) was added dropwise to an aqueous solution (4 mL) of $[V(OH_2)_6]SO_4$ (400 mg, 1.57 mmol) at room temperature. After the addition, the solution was stirred at room temperature for 1 day and dark-violet **5** formed. It was collected by filtration, washed with H_2O, and dried in vacuo (Yield: 250 mg; 91%). Anal. Calcd for $C_2H_4O_6V$: C, 13.73; H, 2.30. Found: C, 13.78; H, 2.42. FT-IR (KBr): 3393 (ν_{OH}), 1652 (ν_{OH}), 1626 (ν_{CO}), 1349, 1307, 823, 480 cm^{-1}. The TGA shows a 20.6% weight loss ≤260 °C, corresponding to the loss of two coordinated water molecules per unit formula, and decomposition starts at 290 °C.

Table 1. Crystallographic Data for $K_3[V(ox)_3] \cdot 3H_2O$, **1**

formula	$C_6H_6K_3O_{15}V$
M_r	486.35
crystal system	monoclinic
space group	$P2_1/c$
a (Å)	7.730(1)
b (Å)	19.944(1)
c (Å)	10.262(1)
α (deg)	90
β (deg)	107.671(1)
γ (deg)	90
V (Å^3)	1507.4(2)
Z	4
D_{calc} (g cm^{-3})	2.143
T (K)	213(2)
λ (Å)	0.71073
μ (mm^{-1})	1.568
R_1 [a] (4σ data)	0.0292
wR_2 [b] (4σ data)	0.0772

[a] $R_1 = \sum||F_o| - |F_c||/\sum|F_o|$. [b] $wR_2 = [\sum w(F_o^2 - F_c^2)^2/\sum w(F_o^2)^2]^{1/2}$.

X-ray Diffraction. Intensity data for **1** were collected with a Bruker SMART automatic diffractometer (Mo Kα, $\lambda = 0.71073$ Å, graphite monochromator). The raw data were processed to give structure factors using the SAINT program.[18] The intensities were corrected for absorption using the Bruker SADABS program[19a] with the transmission factors ranging from 0.65 to 0.86. The crystal structure was solved by the direct methods[19b] and refined by full-matrix least-squares refinement using the SHELXL97 computer program.[19c] The positions of all nonhydrogen atoms were refined with anisotropic displacement factors. All hydrogen atoms of water molecules were located and refined with isotropic thermal parameters. The crystallographic data of **1** are summarized in Table 1.

Results and Discussion

Synthesis and Characterization. Layered (2-D) {[N(*n*-Bu)$_4$][Mn^{II}V^{III}(ox)$_3$]}$_n$, **2**, was prepared in near quantitative yield by mixing an equimolar aqueous solution of $K_3[V^{III}(ox)_3] \cdot 3H_2O$ and $MnCl_2 \cdot 4H_2O$ to an aqueous solution of [N(*n*-Bu)$_4$]Br at room temperature in the air.

Layered {[N(*n*-Bu)$_4$][V^{II}Cr^{III}(ox)$_3$]}$_n$, **3**, was prepared as a dark-violet solid by mixing an equimolar aqueous solution of $K_3[Cr(ox)_3] \cdot 3H_2O$ and $[V(OH_2)_6]SO_4$ with an aqueous solution of [N(*n*-Bu)$_4$]Br in an oxygen-free wet box, as V(II) and **3** are very sensitive to air, but not moisture. Hence, as discussed by Okawa, product formation of both **2** and **3** does not occur unless the bulky cation is used as a template.[9b] When **3** is exposed to air for a few minutes, the color becomes blue-green, and a new strong peak at 998 cm^{-1} appears, indicating formation of V^{IV}=O due to oxidation. In an attempt to obtain {[N(*n*-Bu)$_4$][Cr^{II}V^{III}(ox)$_3$]}$_n$, $K_3[V(ox)_3] \cdot 3H_2O$, $CrCl_2$, and [N(*n*-Bu)$_4$]Br were reacted, but dark-violet

(17) Miller, J. S.; Kravitz, S. H.; Kirschner, S.; Ostrowski, P.; Nigrey, P. J. *J. Chem. Educ.* **1977**, *55*, 181.

(18) *Saint Plus*, v. 6.02; Bruker Analytical X-ray: Madison, WI, 1999.

(19) (a) Sheldrick G. M. *SADABS: Program for Empirical Absorption of Area Detector Data*; University of Göttingen: Göttingen, Germany, 1996. (b) Sheldrick G. M. *Acta Crystallogr.* **1990**, *A46*, 467. (c) Sheldrick G. M. *SHELXL97, Program for the Crystal Structure Refinement*; University of Göttingen, Germany, 1997.

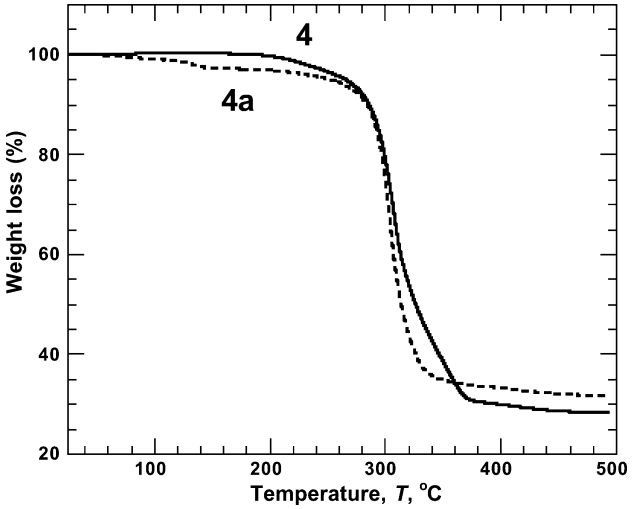

Figure 2. TGA of **4** and **4a**.

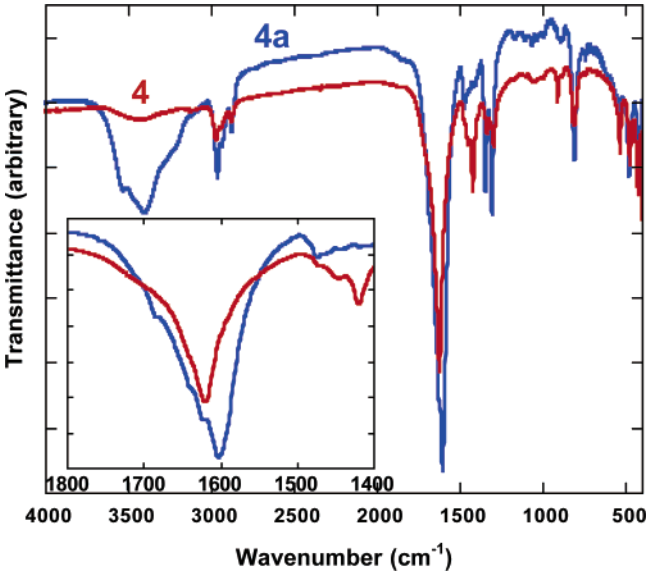

Figure 3. IR spectra of **4** and **4a**.

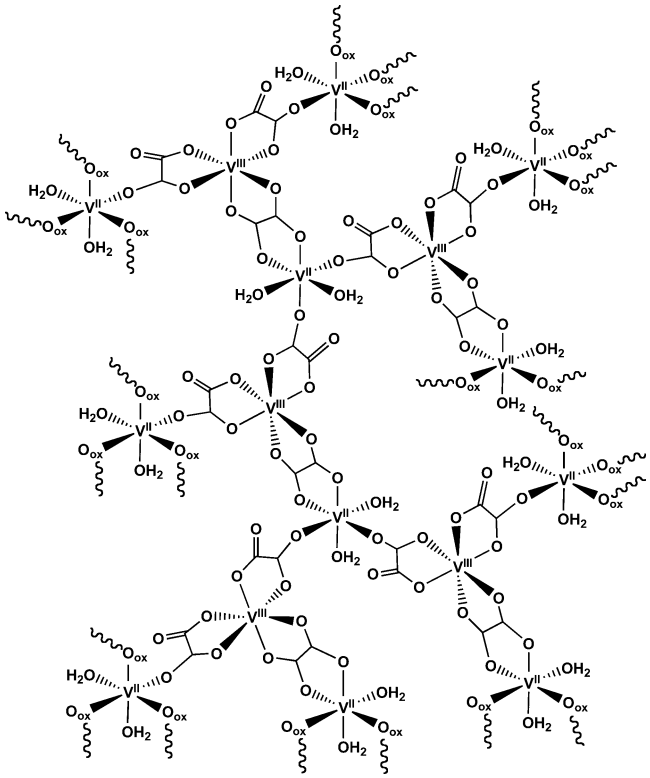

Figure 4. Proposed structure for **4a**.

3 was isolated as characterized by its color, IR, and magnetic data. Alternatively, **3** can be formed from the reaction of $K_3[V(ox)_3]\cdot 3H_2O$ and $[Cr^{II}(OH_2)_6]SO_4$ with an aqueous solution of $[N(n\text{-}Bu)_4]Br$. In accord with the 0.15 V greater reduction potential of $Cr^{III}(aq)$ with respect to $V^{III}(aq)$,[20] $[Cr^{II}V^{III}(ox)_3]^- \rightarrow [V^{II}Cr^{III}(ox)_3]^-$ occurs.

$\{[N(n\text{-}Bu)_4][V^{II}V^{III}(ox)_3]\}_n$ (4). Layered **4** was sought from the reaction of an equimolar aqueous solution of $K_3[V(ox)_3]\cdot 3H_2O$ and $[V^{II}(OH_2)_6]SO_4$ with an aqueous solution of $[N(n\text{-}Bu)_4]Br$. Upon standing for 15 h a dark-violet solid with strong, sharp IR absorptions at 1603 and 1626 cm^{-1} assignable to ν_{CO} was isolated. This doublet was at variance with the observation of single ν_{CO} absorptions[9] for related compounds, including **2** (1630 cm^{-1}) and **3** (1619 cm^{-1}). This suggested the presence of two species, although reduction of the local crystal symmetry might lead to a doublet. Subsequent temperature-dependent magnetic studies revealed two peaks at 9 and 23 K, which are anomalous as peaks are not expected, and certainly not two (vide infra). Assuming that two species were present, the reaction time was altered and subsequently two species, **4** and **4a**, each with a single ν_{CO} absorption and one peak in the magnetic data were isolated.

The composition of **4** was determined from the elemental analysis, IR, powder X-ray diffraction, and TGA data to be anhydrous $\{[N(n\text{-}Bu)_4][V^{II}V^{III}(ox)_3]\}_n$. Unlike **4**, water is evident in the IR spectrum (ν_{OH}: 3393, 1652 cm^{-1}) of **4a**. Furthermore, the TGA data of **4a** (Figure 2) also indicate the presence of coordinated water molecules, and the 5.1% mass loss below 250 °C is attributed to 2 equiv of water. On the basis of these observations and the %C, %H, and %N, **4a** is proposed to be $\{[N(n\text{-}Bu)_4][V^{II}V^{III}(ox)_3(H_2O)_2]\}_n\cdot 2.5H_2O$.

Each V^{III} in **4** is coordinated by six oxygen atoms of three oxalates, Figure 1. The differences in the IR spectra between **4** and **4a** (Figure 3) indicate that **4a** has coordinated water and two different carbonyls. Thus, while most oxalato ligands chelate-bridge V^{II} and V^{III} sites and have a typical ν_{CO} at 1624 cm^{-1}, some oxalato ligands chelate to the V^{III} site and the O^- coordinates to a V^{II} site, which still has water coordinated to it, Figure 4. This isolated intermediate, **4**, forms from the aqueous reaction of $[V^{II}(OH_2)_6]^{2+}$ and $[V^{III}(ox)_3]^{3-}$, which initially must proceed with loss of water and coordination of an unbound oxalato oxygen. The 1603 cm^{-1} ν_{CO} absorption is attributed to a similar, but different CO bonding mode as proposed.[21] While absorption is expected to be rapid, as occurs for other $[M^{III}(ox)_3]^{3-}$ (M =

(20) Lide, D. R., Ed. *Handbook of Chemistry and Physics*, 81st ed.; CRC Press: Boca Raton, 2000; pp 8-21−8-26.

(21) Nakamoto, K. *Infrared and Raman Spectra of Inorganic and Coordination Compounds*, 5th ed.; John Wiley and Sons, Inc.: New York, 1997; Part B, pp 74−77.

Fe, Cr),[9] due to the lability for V^{II} and the reaction occurring in water shifting the equilibrium toward V^{II} aquo species, complete loss of water forming **4** is sufficiently slow and with precipitation of this species as **4a** is isolated. Thus, as the reaction proceeds, kinetically formed **4a** transforms into the expected thermodynamically stable $\{[N(n\text{-}Bu)_4][V^{II}V^{III}(ox)_3]\}_n$ (**4**), by releasing the coordinated water molecules.

After 3 days, **4** ($\nu_{CO} = 1621$ cm^{-1}) formed in 64% yield, while **4a** ($\nu_{CO} = 1603$ and 1624 cm^{-1}) (Figure 3) was obtained within 2−3 h in low yield. Contrary to **2**, **3**, and **4** with a single ν_{CO} absorption, **4a** has two ν_{CO} bands indicating two different oxalate-bridging modes. One is fully coordinated as tetradentate ligand (1624 cm^{-1}), and the other is coordinated as tridentate ligand with one free oxygen atom (1603 cm^{-1}).[21] Both compounds are very air, but not moisture, sensitive. When they are exposed to air for a few minutes, **4** and **4a** become dark green, and new strong peaks at 997 and 991 cm^{-1} appear, respectively, indicating that the V^{II} is oxidized to vanadyl (V^{IV}═O). Unlike **4**, **4a** exhibits a broad ν_{OH} absorption at 3528 cm^{-1} indicative of water, which is also not present for anhydrous-layered **2** and **3**.

Attainment of $\{[N(n\text{-}Bu)_4][M^{II}V^{III}(ox)_3]\}_n$ (M^{II} = Fe, Co, Ni, Cu, Zn), while attempted several times via the reactions of solutions $K_3[V(ox)_3]\cdot 3H_2O$ and $FeCl_2\cdot 4H_2O$, $Co(NO_3)_2\cdot 6H_2O$, $Ni(NO_3)_2\cdot 6H_2O$, $Cu(NO_3)_2\cdot 3H_2O$, and $Zn(NO_3)_2\cdot 6H_2O$, respectively, with $[N(n\text{-}Bu)_4]Br$, was unsuccessful. However, $[M^{II}(ox)(OH_2)_2]_n$ (M = Cr,[22] Fe,[23−25a] Co,[24,25b,26,27] Ni,[24,25b,26] Cu,[24] Zn[24,25b,26]) was isolated. This is attributed to the lability of $[V(ox)_3]^{3-}$, and subsequent formation of antiferromagnetically coupled $M^{II}(ox)(OH_2)_2$.[23,26] $[V^{II}(ox)(OH_2)_2]_n$ (**5**), however, has yet to be reported, and while it is a byproduct in the formation of $\{[N(n\text{-}Bu)_4][V^{II}V^{III}(ox)_3]\}_n$, **4**, it was isolated from the aqueous reaction of Na_2ox and $[V^{II}(OH_2)_6]^{2+}$.

One-dimensional **5** is also sensitive to air and not moisture. When **5** is exposed to air, a weak peak at 989 cm^{-1} appears, indicative of the oxidation of V^{II} to vanadyl (V═O). Contrary to **3**, **4**, and **4a**, oxidation of **5** occurred very slowly.

Attempts to prepare $\{[N(n\text{-}Bu)_4][V^{II}Fe^{III}(ox)_3]\}_n$ and $\{[N(n\text{-}Bu)_4][Cr^{II}Fe^{III}(ox)_3]\}_n$ by mixing an equimolar aqueous solution of $K_3[Fe(ox)_3]\cdot 3H_2O$ with an aqueous solution of V^{II} and/or Cr^{II} were made. Prior to addition of $[N(n\text{-}Bu)_4]$-Br, precipitates of $[Fe^{II}(ox)(OH_2)_2]_n$ and $[Cr^{II}(ox)(OH_2)_2]_n$ composition formed.

The TGA trace of **1** shows a weight loss of 11.1% at 122 °C, corresponding to the loss of lattice water molecules. Compounds **2**, **3**, and **4** do not have water, and show the onset of decompositions at 280, 215, and 220 °C, and complete decomposition occurs abruptly at 345, 310, and 280 °C, respectively for **2**, **3**, and **4**. The TGA trace of **4a** shows a weight loss of 5.1% at 250 °C, corresponding to the loss of two water molecules per unit formula (Figure 2). No chemical decomposition was observed below 260 °C. The TGA trace of **5** shows a weight loss of 18.9% at 260 °C, corresponding to the loss of two coordinated water molecules (20.6%) per unit formula, and the onset of decomposition at 290 °C. Compounds **2**−**5** are insoluble in water, however, $K_3[V(ox)_3]\cdot 3H_2O$ (**1**) and $K_3[Cr(ox)_3]\cdot 3H_2O$ are very soluble in water.

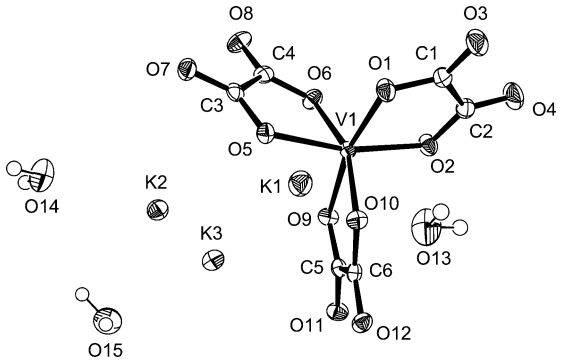

Figure 5. ORTEP drawing of $K_3[Cr(ox)_3]\cdot 3H_2O$, **1**, with atomic numbering scheme. The atoms are represented by 50% probability thermal ellipsoids.

Table 2. Selected Bond Distances, Å, and Angles, Deg, for $K_3[V(ox)_3]\cdot 3H_2O$, **1**

V1−O1	1.995(1)	O1−C1	1.286(2)
V1−O2	2.006(1)	O2−C2	1.294(2)
V1−O5	2.049(1)	O3−C1	1.222(2)
V1−O6	1.969(1)	O4−C2	1.216(2)
V1−O9	2.051(1)	C1−C2	1.544(2)
V1−O10	1.973(1)		
O1−V1−O2	80.34(5)	O2−V1−O10	101.37(5)
O1−V1−O5	87.89(5)	O5−V1−O6	80.05(5)
O1−V1−O6	102.40(5)	O5−V1−O9	102.56(5)
O1−V1−O9	167.18(5)	O5−V1−O10	87.14(5)
O1−V1−O10	93.19(5)	O6−V1−O9	86.90(5)
O2−V1−O5	165.77(5)	O6−V1−O10	159.33(5)
O2−V1−O6	94.62(5)	O9−V1−O10	80.09(4)
O2−V1−O9	90.22(5)		

X-ray Crystallography. Compound **1** crystallizes in the monoclinic $P2_1/c$ space group. The room temperature unit cell parameters were previously reported ($a = 7.810$ Å, $b = 20.010$ Å, $c = 10.350$ Å, $\beta = 108.55°$, $V = 1533.45$ Å^3). However, due to poor crystal quality ($R = 15\%$), the structure could not determined.[28] The structure was redetermined at −60 °C ($R = 2.92\%$). An ORTEP atom labeling drawing of **1** is shown in Figure 5, and Table 2 lists the selected bond distances and angles. As expected, V^{III} is coordinated with six oxygen atoms of three oxalate dianions as a trigonally distorted octahedron, which has approximately D_3 symmetry. The space group and unit cell parameters of **1** are similar to those reported for $K_3[M(ox)_3]\cdot 3H_2O$ (M = Al, Fe, Cr); thus, **1** is isomorphous to these compounds.[14a] In contrast, $K_3[Co(ox)_3]\cdot 3H_2O$ has a different unit cell,[29] and $K_3[Ru(ox)_3]\cdot 4.5H_2O$ also crystallizes in different $P\bar{1}$ motif with respect to **1** due to the lattice water molecules.[30] Nonetheless, in all

(22) Nikumbh, A. K.; Rahman, M. M.; Aware, A. D. *Thermochim. Acta* **1990**, *159*, 109.
(23) Wrobleski, J. T.; Brown, D. B. *Inorg. Chem.* **1979**, *18*, 2738.
(24) Nagase, K.; Sato, K.; Tanaka, N. *Bull. Chem. Soc. Jpn.* **1975**, *48*, 439.
(25) (a) Deyrieux, R.; Peneloux, A. *Bull. Soc. Chim.* **1969**, 2675. (b) Deyrieux, R.; Berro, C.; Peneloux, A. *Bull. Soc. Chim.* **1973**, 25.
(26) van Kralingen, C.; van Ooijen, J. A. C.; Reedijk, J. *Transition Met. Chem.* **1978**, *3*, 90.
(27) Garcia-Coucerio, U.; Castillo, O.; Luque, A.; Beobide, G.; Roman, R. *Inorg. Chim. Acta* **2004**, *357*, 339.
(28) Fenn, R. H.; Graham, A. J.; Gillard, R. D. *Nature* **1967**, *213*, 1012.
(29) Okazaki, H.; Kushi, Y.; Yoneda, H. *J. Am. Chem. Soc.* **1985**, *107*, 4183.
(30) Faure, R.; Duc, G.; Deloume, J.-P. *Acta Crystallogr.* **1986**, *C42*, 982.

cases the metal ion is octahedrally surrounded by three oxalato ligands in nearly D_3 local symmetry.

The V−O_{ox} distances range from 1.973(1) to 2.051(1) Å, and average 2.007(1) Å. The average ligand bite distances of coordinated five-membered chelate rings and noncoordinated free oxalates are 2.585 and 2.794 Å, respectively. The separation of V···V between the $[V(ox)_3]^{3-}$ complex ions is 6.929 Å. The shortest $K^+ \cdots K^+$ interaction distance is 3.783 Å. All potassium cations are involved in ionic interactions with lattice water molecules (K1···O13 = 2.715, K1···O14 = 2.777, K2···O14 = 2.635, K3···O13 = 2.888, K3···O15 = 2.952 Å). In addition, the lattice water molecules form hydrogen bonds with the other lattice water molecule [O13···O15($-x + 1, -y + 1, -z + 1$) = 2.697 Å, O14···O15 = 2.959 Å].

Compound **2** crystallizes in the hexagonal system, and the unit cell parameters were obtained by single-crystal X-ray diffraction as follows, i.e., $a = b = 9.467$ Å, $c = 52.276$ Å, $\alpha = \beta = 90°$, $\gamma = 120°$, $V = 4057.02$ Å^3, but the crystal structure could not be determined due to the poor crystallinity. These parameters are in good agreement with $\{[N(n\text{-}Bu)_4][Mn^{II}Cr^{III}(ox)_3]\}_n$ ($a = b = 9.397$ Å, $c = 53.580$ Å, $\alpha = \beta = 90°$, $\gamma = 120°$, $V = 4097.43$ Å^3, $R6_c$)[31] and $\{[N(n\text{-}Bu)_4][Mn^{II}Co^{III}(ox)_3]\}_n$ ($a = b = 9.242$ Å, $c = 54.524$ Å, $\alpha = \beta = 90°$, $\gamma = 120°$, $V = 4033.21$ Å^3, $R6_c$).[12] Hence, **2** is isomorphous to $\{[N(n\text{-}Bu)_4][Mn^{II}Cr^{III}(ox)_3]\}_n$ and $\{[N(n\text{-}Bu)_4][Mn^{II}Co^{III}(ox)_3]\}_n$.

Compound **3** also crystallizes in the hexagonal system with $a = b = 9.337$ Å, $c = 17.894$ Å, $\alpha = \beta = 90°$, $\gamma = 120°$, $V = 1351.11$ Å^3. These parameters are in good agreement with $\{[N(n\text{-}Bu)_4][Mn^{II}Fe^{III}(ox)_3]\}_n$ ($a = b = 9.482$ Å, $c = 17.827$ Å, $\alpha = \beta = 90°$, $\gamma = 120°$, $V = 1388.10$ Å^3, $P6_3$).[10a] Thus, **3** is isomorphous to $\{[N(n\text{-}Bu)_4][Mn^{II}Fe^{III}(ox)_3]\}_n$. The interlayer separations between the 2-D anionic layers of $\{[N(n\text{-}Bu)_4][Mn^{II}Cr^{III}(ox)_3]\}_n$ and $\{[N(n\text{-}Bu)_4][Mn^{II}Fe^{III}(ox)_3]\}_n$ were 8.95 and 8.99 Å, respectively. Although these two compounds have different cell parameters and space groups, they both form the 2-D hexagonal motif (Figure 1) albeit the former with six anionic layers and the latter with two anionic layers per unit cell. In all cases similar interlayer separations of ~9 Å are observed.

Compound **4** crystallizes in the hexagonal system with $a = b = 9.394$ Å, $c = 17.710$ Å, $\alpha = \beta = 90°$, $\gamma = 120°$, $V = 1353.47$ Å^3. These parameters are in good agreement with those of **3** and $\{[N(n\text{-}Bu)_4][Mn^{II}Fe^{III}(ox)_3]\}_n$.[11a] Thus, **4** is also isomorphous to **3** and $\{[N(n\text{-}Bu)_4][Mn^{II}Fe^{III}(ox)_3]\}_n$.[11a]

The X-ray powder diffraction (XRPD) pattern of **4a** is very different from that of **4** with respect to the positions and broadness of peaks. Most of the peaks in **4a** are broad except for the peak of $2\theta = 8.890°$ (9.939 Å), indicating that the network structure of **4a** is disordered significantly. Determination of the unit cell parameters could not be done however, due to the broad, weak X-ray powder diffraction peaks that could not be indexed even when using synchrotron radiation.[32] The XRPD pattern of **4** was clearly shown in the diffraction peak indicating 2-D interlayer separation at $2\theta = 9.843°$ (8.979 Å) while no peak(s) at $2\theta \sim 9.84°$ (8.98 Å) were evident in the XRPD pattern of **4a**. Thus, the structures of **4** and **4a** appear similar, but the structure of **4a** in unknown.

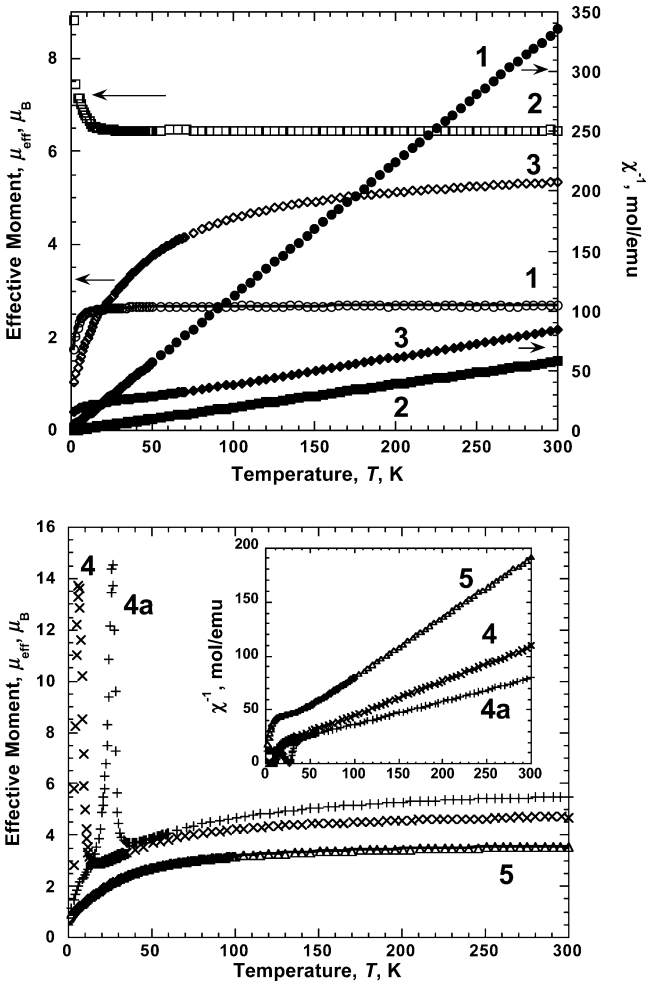

Figure 6. $\mu_{eff}(T)$ and $\chi^{-1}(T)$ for **1** (○, ●), **2** (□, ■), **3** (◇, ◆), **4** (×), **4a** (+), and **5** (△). The solid lines represent the best-fit curves to the eq 2 for **1** and eq 4 for **5**.

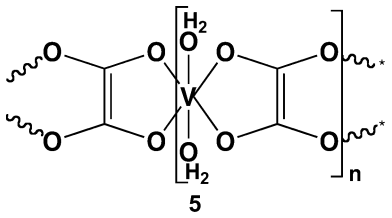

Magnetic Properties. The magnetic susceptibilities, χ, of **1**−**4**, **4a**, and **5** were measured on powdered samples in an applied field of 500, 200, 50, 300, 300, and 200 Oe, respectively, between 2 and 300 K, and are plotted as $\chi(T)$ and $\mu_{eff}(T)$ $\{\mu_{eff} = [8\chi T]^{1/2}\}$, Figure 6. Assuming a g-value of 1.894, as reported for $[Cs(OH_2)_6][V(OH_2)_6](SO_4)_2$,[33] a 300 K μ_{eff} of 2.68 is expected, and is observed for **1**,[34] Figure

(31) Shilov, G. V.; Atovmyan, L. O.; Ovanesyan, N. S.; Pyalling, A. A.; Bottyan, L. *Koord. Khim.* **1998**, *24*, 305.

(32) Her, J.-H.; Stephens, P. W., private communication.

(33) Tregenna-Piggott, P. L. W.; Spichiger, D.; Carver, G.; Frey, B.; Meier, R.; Weihe, H.; Cowan, J. A.; Mclntyre, G. J.; Zahn, G.; Barra A.-L. *Inorg. Chem.* **2004**, *43*, 8049.

6a. $\mu_{eff}(T)$ decreases slightly with decreasing temperature to 2.61 μ_B at 20 K, followed by an abrupt decrease to 1.74 μ_B at 2.0 K, indicating either an intermolecular interaction (θ) or a zero-field splitting (D) or both. Using the Hamiltonian, eq 1, the expression for $\chi(T)$, eq 2, was derived,[35] and the data were fit to eq 2 for $\chi(T,D,\theta)$ where N, μ_B, k_B, and θ are Avogadro's number, the Bohr magneton, the Boltzmann constant, and the Weiss constant, respectively, with D for the V^{III} ion having a value of 3.84 cm^{-1} ($D/k_B = 5.53$ K), $\theta = -1.11$ K and $g = 1.895$, Figure 6a. These values are in good agreement with $[Cs(OH_2)_6][V(OH_2)_6](SO_4)_2$, i.e., $D = 4.87$ cm^{-1} ($D/k_B = 7.01$ K) and $g = 1.894$.[33] The θ value is comparable to -1.12 K for the Weiss constant based on the Curie−Weiss equation, $\chi \propto (T - \theta)^{-1/2}$. Thus, as expected, **1** possesses an $S = 1$ ground state with $D = 3.84$ cm^{-1} ($D/k_B = 5.53$ K). The significant positive D-value is an order of magnitude greater than the D-values of 0.18[36a] and 0.42[36b] cm^{-1}, respectively, reported for $K_3[M(ox)_3]\cdot 3H_2O$ (M = Fe, Cr). This is attributed to the small zero-field splitting of the ground state, inherent to Kramers ions for the latter ions. More importantly, $[V^{III}(ox)_3]^{3-}$ might be a suitable component for developing new single molecule magnets.[37]

$$H = g_u \mu_B \mathbf{S}_u H_u + D[\mathbf{S}_z^2 - S(S+1)/3] - zJ\langle S_z\rangle \mathbf{S}_z \quad (1)$$

$$\chi = \frac{2Ng^2\mu_B^2}{3k_B(T-\theta)}\left[\frac{\exp(-D/T)}{1+2\exp(-D/T)} + \frac{2T}{D}\left(\frac{1-\exp(-D/T)}{1+2\exp(-D/T)}\right)\right] \quad (2)$$

The 300 K magnetic moment of **2** is 6.44 μ_B, and it is almost constant with decreasing temperature until 20 K (Figure 6a). The value of μ_{eff} at room temperature is in accord with 6.49 μ_B expected for independent $S = 1$ V^{III} ($g = 1.894$) and $S = 5/2$ Mn^{II} ($g = 2$) spins. Below 20 K, $\mu_{eff}(T)$ increases steeply to 8.83 μ_B at 2 K. This value of μ_{eff} exceeds the 7.94 μ_B expected for the isolated Mn^{II} ($S = 5/2$) and V^{III} ($S = 1$) ions, suggestive of significant ferromagnetic interactions. Above 2 K $\chi^{-1}(T)$ can be fit to the Curie−Weiss expression with $\theta = +0.82$ K, indicating weak ferromagnetic interactions (Figure 6a).

To ascertain if **2** magnetically orders the AC susceptibility, $\chi'(T)$ and $\chi''(T)$, were measured below 10 K (Figure 7). $\chi'(T)$ increases continuously with decreasing the temperature to 2 K, irrespective of frequencies (10, 100, 1000 Hz) without reaching a maximum. This suggests that **2** magnetically orders below 2 K. In contrast, $\chi''(T)$ is zero almost in the temperature range, indicating that the ordering is antiferromagnetic.

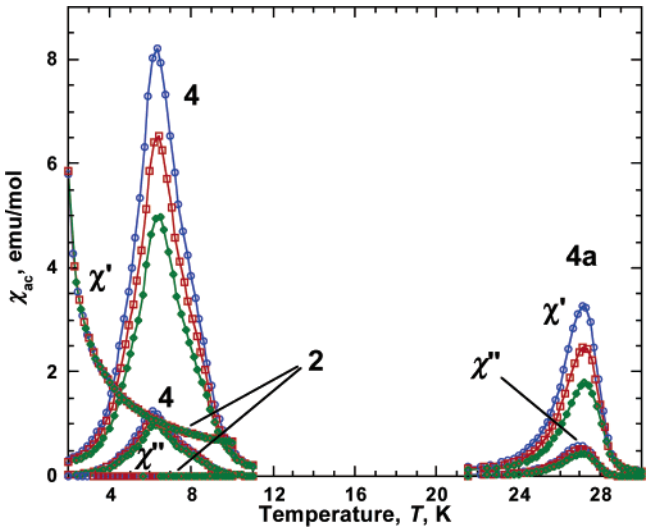

Figure 7. $\chi'(T)$ and $\chi''(T)$ for **2**, **4**, and **4a** at 10 (○), 100 (□), and 1000 (◆) Hz.

To control T_cs, we have prepared $\{[N(n\text{-}Bu)_4][Mn^{II}Cr_x^{III}V_{1-x}^{III}(ox)_3]\}_n$ ($x = 0.5$, 0.8). When x was 0 (**2**) and 1, the T_cs were <2 K and ca. 6 K,[9] respectively. By increasing x, T_c should increase to 6 K, and as x increases, the magnetization and the temperature at which a maximum in $\mu_{eff}(T)$ occurs increases, i.e., it is at 3.03 K for $x = 0.5$ and 4.65 K for $x = 0.8$. Furthermore, for $x = 0.8$, the maximum in $\chi'(T)$ occurs at 5.0 K, while $\{[N(n\text{-}Bu)_4][Mn^{II}V^{III}(ox)_3]\}_n$ (**2**) does not have a maximum. Thus, by varying the composition of Cr, x, the T_cs can be controlled between 2 and 6 K. This behavior has been observed for the related $\{[N(n\text{-}Bu)_4][Fe^{II}Fe^{III}{}_xCr^{III}{}_{1-x}(ox)_3]\}_n$ family of magnets.[11c]

Compound **3** has a 300 K effective magnetic moment of 5.33 μ_B that decreases monotonically with decreasing temperature to 1.04 μ_B at 2 K. This is less than 5.48 μ_B expected for independent $g = 2$ $S = 3/2$ V^{II} and $S = 3/2$ Cr^{III} spins indicative of strong antiferromagnetic interaction. Above 20 K, the data can be fit the Curie−Weiss expression with $\theta = -116$ K, in accord with a strong antiferromagnetic interaction (Figure 6), but not ordering, as also occurs for $\{[N(n\text{-}Bu)_4][Cr^{II}Cr^{III}(ox)_3]\}_n$, which possesses a weaker antiferromagnetic coupling, i.e., $\theta = -12.7$ K, and does not magnetically order.[38]

Compounds **4** and **4a** have effective magnetic moments of 4.69 and 5.50 μ_B at 300 K. The μ_{eff} values decrease upon cooling to minima of 2.87 μ_B at 17 K and 3.67 μ_B at 37 K, and then increase to maxima of 13.7 μ_B at 6.1 K and 14.5 μ_B at 27 K, for **4** and **4a**, respectively, Figure 6b. This is indicative of ferrimagnetic behavior. $\chi^{-1}(T)$ values in the temperature ranges of 20−300 K for **4** and 40−300 K for **4a** can be fit to the Curie−Weiss expression with $\theta = -45$ and -76 K, respectively, indicating strong antiferromagnetic couplings.

The 2 K field dependence of the magnetization, $M(H)$, shows rapid rise with increasing applied field, H, indicative

(34) μ_{eff} values for **1** were 2.80 μ_B at 303 K and 2.75 μ_B at 85 K. (a) Figgis, B. N.; Lewis, J.; Mabbs, F. *J. Chem. Soc.* **1960**, 2480. (b) Machin, D. J.; Murray, K. S. *J. Chem. Soc.* (*A*) **1967**, 1498.

(35) Kahn, O. *Molecular Magnetism*; VCH: Weinheim, Germany, 1993; pp 17−29.

(36) (a) Collison, D.; Powell, A. K. *Inorg. Chem.* **1990**, *29*, 4735. (b) Bai, L.-J. *Bopuxue Zazhi* **2001**, *18*, 215.

(37) (a) Christou, G.; Gatteschi, D.; Hendrickson, D. N.; Sessoli, R. *MRS Bull.* **2000**, *25(no. 11)*, 66. (b) Gatteschi, D.; Hendrickson, D. N.; Sessoli, R. *Angew. Chem., Int. Ed.* **2003**, *42*, 268.

(38) Nuttall, C. J.; Bellitto, C.; Day, P. *J. Chem. Soc., Chem. Commun.* **1995**, 1513.

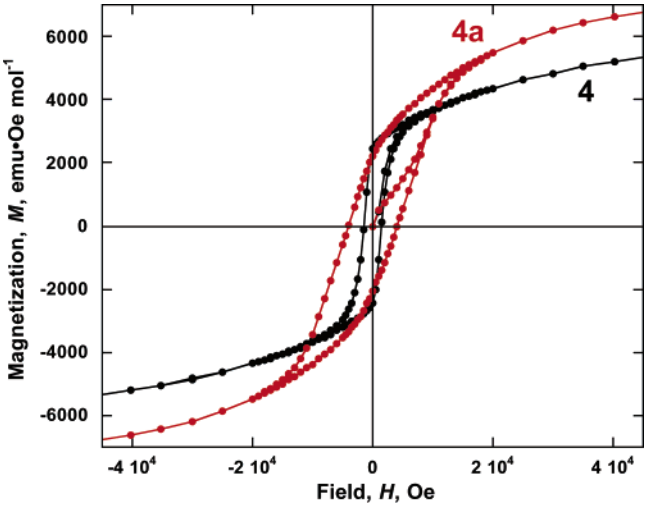

Figure 8. 2 K hysteresis, $M(H)$, of **4** and **4a**.

of magnetic ordering for **4** and **4a** (Figure 8). The magnetizations at 5 T are 5575 and 6960 emu·Oe/mol for **4** and **4a**, respectively, but while still gradually rising with increasing applied field they are in accord with the expectation of 5585 emu·Oe/mol for antiferromagnetic coupling leading to ferrimagnetic ordering, but substantially less than 27 925 emu·Oe/mol expected for ferromagnetic ordering.

At 2 K the remanant magnetizations are 2440 and 2230 emu Oe mol^{-1} and the coercive fields, H_{cr}, are 1460 and 4060 Oe for **4** and **4a**, respectively (Figure 8). These values exceed those reported for $[M^{II}Cr^{III}(ox)_3]^-$ (H_{cr} = 20−320 Oe)[9b] and $(NBu_4)[Fe^{II}Fe^{III}(ox)_3]$ (H_{cr} = ∼580 Oe), but is lower than 11 500 Oe reported for $(PPh_4)[Fe^{II}Fe^{III}(ox)_3]$.[39] The FCM (field-cooled magnetization) and ZFCM (zero-field-cooled magnetization) for **4** and **4a** were measured under a weak magnetic field (5 Oe). The FCMs in both compounds show sharp onsets in the magnetization at 11 and 30 K, their T_c's. The ferrimagnetic bifurcation temperatures (T_b) determined by the divergence between the FC and ZFC magnetizations are 9.5 and 28 K, respectively.

The peaks in both the in-phase, real, $\chi'(T)$, and out-of-phase, imaginary, $\chi''(T)$, components of the AC susceptibility, $\chi_{ac}(T)$ for **4** and **4a** are characteristic of magnetic ordering (Figure 7). Both **4** and **4a** clearly show a frequency dependence, as evidenced by ϕ values $\{\phi = \Delta T_f / [T_f\, \Delta(\log f)]$, where T_f is the temperature of the peak in the lowest frequency (10 Hz) data, and χ' is the frequency in Hz, and the greater the frequency dependence the larger the value of $\phi\}$ of 0.011 for **4** and 0.002 for **4a**. This is indicative of spin-glass-like behavior.[40] The glass transition temperatures extracted from the peak position at 10 Hz $\chi'(T)$ data are 6.3 and 27 K, respectively.

Compound **5** has a 300 K effective magnetic moment of 3.54 μ_B that decreases monotonically with decreasing temperature to 0.94 μ_B at 2 K (Figure 6b). The $\chi^{-1}(T)$ between 20 and 300 K can be fit to the Curie−Weiss expression with

Table 3. Magnetic Parameters for Oxalato-Bridged M(II) (M = V, Cr, Mn, Fe, Co, Ni) 1-D Chains

compound	g	J, cm^{-1}	θ	ref
$[V(ox)(H_2O)_2]_n$ (**5**)	1.95	−4.94	−49	this work
$[Cr(ox)(H_2O)_2]_n$	μ_{eff} = 4.65 μ_B (300 K)			22
$[Mn(ox)(H_2O)_2]_n$	2.00	−0.89		42b
$[Fe(ox)(H_2O)_2]_n$	2.23	−3.41	−25.4	42a
$[Co(ox)(H_2O)_2]_n$	6.1, 3.3	−9.3		26
$[Ni(ox)(H_2O)_2]_n$	2.12	−11		26

θ = −49 K, suggestive of a strong antiferromagnetic interaction. Hence, based upon this θ, the spin-only, g = 2, room-temperature effective moment of 3.59 μ_B is expected, which is in excellent agreement with the observed value. The data are modeled with the isotropic V^{II} (S = 3/2) chain spin Hamiltonian, eq 3, for which $\chi(T)$, eq 4 was derived.

$$H = -2J\sum_{i=1}^{n} S_i \cdot S_{i-1} - g\mu_B \sum_{i=0}^{n} H \cdot S_i \qquad (3)$$

$$\chi = \frac{Ng^2\mu_B{}^2 S(S+1)}{3k_B T}\frac{1+U}{1-U} \qquad (4)$$

$$U = \coth\left[\frac{2JS(S+1)}{k_B T}\right] - \left[\frac{k_B T}{2JS(S+1)}\right]$$

The best-fit parameters for the magnetic susceptibility data to eq 4 are g = 1.945 and J = −4.94 cm^{-1} (J/k_B = −7.1 K). At room temperature, V^{II} doped in $CsCdCl_3$ [41a] and $CsCaCl_3$ [41b] has average g values of 1.959 and 1.958, respectively. These values are comparable to that of **5**, $[V(ox)(H_2O)_2]_n$. This antiferromagnetic coupling exceeds those of M = Mn (−0.89 cm^{-1}) and Fe (−3.41 cm^{-1}), but is less than those for M = Co (−9.3 cm^{-1}) and Ni (−11 cm^{-1}),[22,42] Table 3. Hence, oxalate anion mediates antiferromagnetic coupling between two V^{II} ions.

Conclusion

Using the S = 1 $[V(ox)_3]^{3-}$ as well as V(II) and S = 3/2 $[Cr(ox)_3]^{3-}$, V-based layered materials of $\{[N(n\text{-}Bu)_4][Mn^{II}V^{III}(ox)_3]\}_n$ (**2**), $\{[N(n\text{-}Bu)_4][V^{II}Cr^{III}(ox)_3]\}_n$ (**3**), $\{[N(n\text{-}Bu)_4][V^{II}V^{III}(ox)_3]\}_n$ (**4**), and an intermediate in the formation of **4**, $\{[N(n\text{-}Bu)_4][V^{II}V^{III}(ox)_3(H_2O)_2]\}_n \cdot 2.5H_2O$ (**4a**), have been prepared. **2** exhibits strong intralayer ferromagnetic coupling below 20 K, but does not magnetically order, and **3** exhibits a strong antiferromagnetic interaction within the layers. **4** and **4a** order as ferrimagnets at 11 and 30 K, respectively. The T_c for **4a** is substantially greater than that for **4** suggesting that introduction of $M^{II}(OH_2)_2$ linkages at the expense of oxalato linkages for other $[M^{II}M^{III\prime}ox_3]^-$ magnets may enhance might T_c. One-dimensional $[V^{II}(ox)(H_2O)_2]_n$ (**5**) shows antiferromagnetic coupling between the vanadium(II) ions.

The T_cs of mixed-metal tris(oxalato)-based magnets of $[M^{II}M'^{III}(ox)_3]^-$ composition depend on the M^{II} and M^{III} as

(39) Nuttall, C. J.; Day, P. *Chem. Mater.* **1998**, *10*, 3050.
(40) Mydosh, J. *Spin Glasses*; Taylor and Francis, Ltd.: London, 1993; pp 64−76.
(41) (a) Chang, J. R.; McPherson, G. L.; Atwood, J. L. *Inorg. Chem.* **1975**, *14*, 3079. (b) McPherson, G. L.; Freedman, M. R. *Inorg. Chem.* **1976**, *15*, 2299.
(42) (a) Barros, S. de S.; Friedberg, S. A. *Phys. Rev.* **1966**, *141*, 637. (b) Simizu, S.; Friedberg, S. A. *J. Appl. Phys.* **1988**, *63*, 3557.

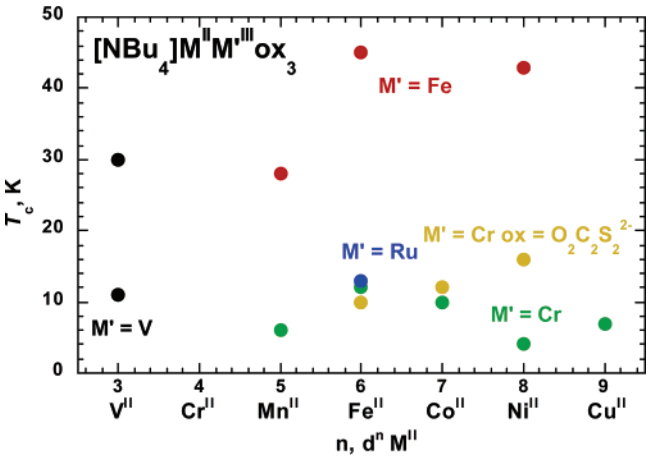

Figure 9. T_c as a function of M^{II} for $[NBu_4][M^{II}M^{III\prime}(ox)_3]$ ($M' = V$, Cr, Fe, and Ru) and $[NBu_4]M^{II}[Cr^{III}(dto)_3]$ (M^{II} = Fe, Co, Ni; dto = $O_2C_2S_2^{2-}$).

illustrated in Figure 9. The T_cs for $M' =$ Ru, Cr, and $[Cr(dto)_3]^{3-}$ (dto = dithioxoalate) are less than 16 K. However, for $M' = Fe^{III}$ the ferrimagnetic T_cs of 2-D layered compounds were increased to ca. 45 K. When the M′ is V, T_cs of V-based ferrimagnets were at 11 and 30 K, respectively, depending on the local composition about the V^{II} ions. Thus, V-based magnets with a T_c higher than those of Cr-based tris(oxalato) ferromagnets have been prepared. Nonetheless, the T_cs are lower than those of Fe-based tris(oxalato) ferrimagnets. Thus, V-based molecule-based magnets with controllable T_cs might be anticipated by using the different metal ions. Furthermore, the intermediate in the formation of **4**, **4a** with fewer $V^{II}oxV^{III}$ linkages, has a substantially greater T_c indicating new families of oxalato-based magnets.

Chain structured $[V^{II}(ox)(H_2O)_2]\}_n$, like $[M^{II}(ox)(H_2O)_2]_n$ (M = Cr, Mn, Fe, Co, Ni), exhibits antiferromagnetic coupling, but not antiferromagnetic ordering (Table 3). The antiferromagnetic coupling for this family ranges from −0.89 ($M = Mn^{II}$) to 11 cm^{-1} ($M = Ni^{II}$), with the V^{II} being intermediate in value.

Acknowledgment. We dedicate this paper to Professor and Dean Hisashi Ōkawa for his pioneering contributions and discovery of trisoxalato-based magnets. The authors appreciate the assistance provided by Atta M. Arif (Utah), and Jae-Hyuk Her and Peter W. Stephens (SUNY, Stony Brook), and the continued partial support by the Department of Energy Division of Materials Science (Grant no. DE-FG03-93ER45504) and Army Research Office (Grant no. DAAD19-01-1-0562).

Supporting Information Available: Crystallographic data (atomic positions, thermal parameters, bond lengths, etc.) for $K_3[V(ox)_3]\cdot 3H_2O$, **1**, in the form of a CIF file. This material is available free of charge via the Internet at http://pubs.acs.org.

IC051373+